NASA TECHNICAL NOTE

NASA TN D-6324

NASA TN D-6324

A STUDY OF LOW-VELOCITY IMPACTS INTO THIN-SHEET ALUMINUM AND NYLON CLOTH

by Robert E. Flaherty

Manned Spacecraft Center
Houston, Texas 77058

NATIONAL AERONAUTICS AND SPACE ADMINISTRATION • WASHINGTON, D. C. • MAY 1971

1. Report No.	2. Government Accession No.	3. Recipient's Catalog No.
NASA TN D-6324		

4. Title and Subtitle	5. Report Date
A STUDY OF LOW-VELOCITY IMPACTS INTO THIN-SHEET ALUMINUM AND NYLON CLOTH	May 1971
	6. Performing Organization Code
7. Author(s)	8. Performing Organization Report No.
Robert E. Flaherty, MSC	MSC S-238
	10. Work Unit No.
9. Performing Organization Name and Address	914-50-18-22-72
Manned Spacecraft Center Houston, Texas 77058	11. Contract or Grant No.
	13. Type of Report and Period Covered
12. Sponsoring Agency Name and Address	Technical Note
National Aeronautics and Space Administration Washington, D.C. 20546	14. Sponsoring Agency Code

15. Supplementary Notes

16. Abstract

Single projectiles were launched at velocities between 0.1 and 0.4 km/sec from a specially designed air gun. The projectiles impacted single and multiple layers of thin-sheet aluminum and nylon cloth to simulate the secondary meteoroid flux in the vicinity of the lunar surface and to define the penetration mechanics of typical spacecraft structures and space-suit materials. The results of these tests have been compared to existing low-velocity-projectile penetration equations, and configurations have been determined for maximum penetration protection.

17. Key Words (Suggested by Author(s))	18. Distribution Statement
* Low-Velocity Impact * Secondary Meteoroids * Spacecraft Material (Impacts On) * Space-Suit Material (Impacts On)	Unclassified-Unlimited

19. Security Classif. (of this report)	20. Security Classif. (of this page)	21. No. of Pages	22. Price*
None	None	27	$3.00

*For sale by the National Technical Information Service, Springfield, Virginia 22151

CONTENTS

TABLES

FIGURES

A STUDY OF LOW-VELOCITY IMPACTS INTO THIN-SHEET ALUMINUM AND NYLON CLOTH

By Robert E. Flaherty
Manned Spacecraft Center

SUMMARY

A specially designed air gun was used to launch 3.175-millimeter (one-eighth inch) diameter steel and glass spherical projectiles at velocities between 0.1 and 0.4 km/sec into materials typically used in the construction of spacecraft and space suits. A uniform sheet thickness (8.89×10^{-2} millimeters (3.5×10^{-3} inches)) of type 1145-H19 aluminum was used throughout the experiment, but the uniform sheets were configured in various ways. Single-sheet targets, layered targets made of single sheets spaced 4.76 millimeters (three-sixteenths inch) apart, and layered targets made of single sheets loosely clamped together to maintain a small separation between the layers were impacted by spherical projectiles with impact velocities between 0.1 and 0.4 km/sec. The results of these tests were compared to existing low-velocity-projectile penetration equations, which showed that, of the configurations tested, the loosely clamped layered target provided the best penetration protection. It was also shown that the percent of the total particle energy absorbed by a given thin sheet decreases as the velocity of the incident particle increases.

Unlike the uniform aluminum sheets, the nylon-cloth target sheets used in the low-velocity-projectile impact experiments varied in thickness and area density. Variations in thread size, thread compactness, type of weave, and chemical treatment of the nylon cloth all contributed to the nonuniform area density among the nylon target sheets. Single and multiple layers of various configurations and compositions were impacted by glass and steel projectiles with impact velocities between 0.1 and 0.4 km/sec. The test results showed that a tight, compact weave is the most efficient energy absorber, that multilayer silicone-treated nylon is a more efficient energy absorber than untreated multilayers of nylon, and that layered targets composed of variable-density materials can be made more efficient energy absorbers if the layers are arranged with the higher density materials on the downstream side of the target.

INTRODUCTION

The secondary-meteoroid flux in the vicinity of the moon presents a low-velocity-particle hazard to near-lunar-surface (maximum altitude, 30 kilometers) and lunar-surface operations. A definition of the ejected lunar material that composes the

secondary-meteoroid environment has been determined from the earth-based experiments discussed in reference 1. The velocity range of the ejecta varies from zero to three times the impacting particle velocity, or from 0 to 216 km/sec. More than 99 percent of the ejected material travels at a velocity less than 1 km/sec, with an average velocity of approximately 0.100 km/sec. Since the ejecta presents a low-velocity-particle penetration hazard to spacecraft, space suits, and structures on the lunar surface, laboratory impact tests are being conducted to define the penetration mechanics of the materials used in the various protection systems. It is the purpose of this report to present experimental data for the ballistic characteristics of aluminum sheet and nylon cloth.

As an aid to the reader, where necessary the original units of measure have been converted to the equivalent value in the Système International d'Unités (SI). The SI units are written first, and the original units are written parenthetically thereafter.

TEST PROCEDURE

A schematic of the compressed-air gun used to accelerate single projectiles is shown in figure 1. The gun is capable of accelerating particles to velocities of 0.1 to 0.4 km/sec. The variation in velocity is obtained by varying either the air pressure that accelerates the projectile or the shear strength of the rupture diaphragm. The velocity is measured with 2.54×10^{-5}-meter (1mil) diameter copper wires inserted into the launch tube. The copper wires are forced into contact by the passage of the sabot, which completes two "make" circuits that, respectively, start and stop an electrical timer. The sabot catcher at the end of the launch tube separates the sabot from the projectile, allowing only the projectile to impact the target. The accuracy of this system was determined to be ± 5 percent.

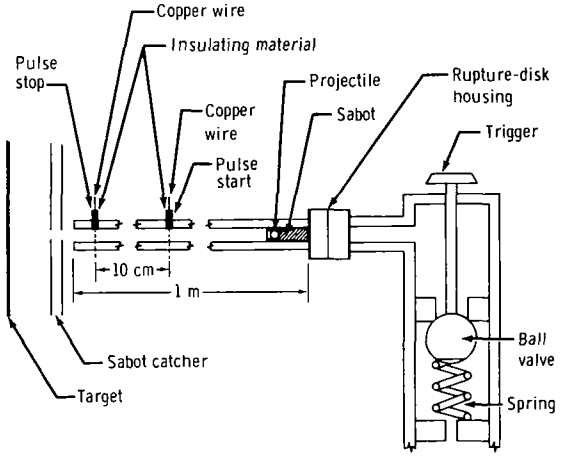

Figure 1. - Air-gun apparatus.

The following target materials and target-material configurations were impacted with 3.175-millimeter (one-eighth inch) diameter glass and steel spheres, which simulate secondary meteoroids. (Most of the work was done with steel projectiles of this size in order to establish upper limits to the anticipated damage caused by the irregularly shaped and lower density secondary-meteoroid particles.)

1. Single and multiple layers of thin-sheet (8.89×10^{-2}-millimeter (3.5×10^{-3} inches)) type 1145-H19 aluminum spaced 4.76 millimeters (three-sixteenths inch) apart and also loosely clamped together to form a laminate

2. Nylon cloth of varying density and surface treatment (table I)

TABLE I. - WOVEN NYLON MATERIALS TESTED

Area density of material		Layers of material tested	Surface treatment of material	Projectile material
kg/m^2	oz/yd^2			
0.082	2.78	1, 2, and 3	None	Steel
.142	4.80	1, 2	Aluminized	Steel
.154	5.21	1	None	Steel
.163	5.50	1	Nylon laminate	Steel
.1791	6.04	1, 2, and 3	None	Steel
.1795	6.05	1 and 2	Aluminized	Steel
.246	8.3	1 and 2	None	Steel
.415	14.0	1 and 2	None	Steel
.415	14.0	1 and 2	Waterproofed	Steel

The multilayer, laminated targets were loosely clamped and fastened to the rear face of the sabot catcher. The equally spaced layers of aluminum were positioned in a modified 35-millimeter-slide holder to obtain constant spacing between each layer. The single-layered and multilayered nylon materials were suspended from a clamp arrangement with a weight attached to the bottom to provide constant tension on each sample.

DISCUSSION OF RESULTS

Multisheet aluminum targets with and without spacing between the layers were impacted with low-velocity projectiles to determine their relative penetration resistance. These targets were impacted with glass and steel spheres to determine the number of sheets perforated for each configuration. The loosely clamped laminate proved to be a more efficient energy absorber than the equally spaced sheets. For each configuration, the number of sheets perforated by the glass and steel projectiles is shown in figure 2.

When multiple layers of the thin-sheet aluminum are impacted simultaneously, as in the loosely clamped laminate, the inner layers must be extruded or compressed

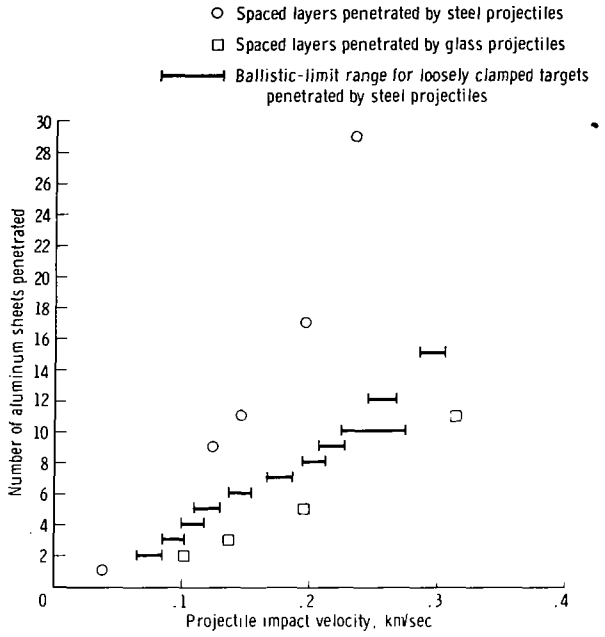

Figure 2. - Penetration of aluminum sheets by glass and steel projectiles.

(or both) before the layers in front are perforated. However, for the evenly spaced aluminum sheets, the projectile penetrates each of the spaced layers separately, and the mechanics of penetration occur separately at each layer. The penetration of a sheet occurs by one of two possible processes, or by a combination of the two processes. The first process occurs when the projectile shears from the target a disk that is approximately the same diameter as the projectile. The second process occurs when the target is extruded by the projectile until the tensile strength of the material is exceeded and the target tears at the projectile-target interface. The second process results in a large extrusion accompanied by radial tearing on the downstream surface of the target. The velocity of the projectile determines which process will dominate.

The results of the two processes are shown in figure 3. Figure 3(a) shows a single sheet of aluminum penetrated by a steel projectile with an impact velocity of 0.300 km/sec. (Note the small target interaction area.) Figure 3(b) shows an identical target penetrated by a glass projectile with an impact velocity of 0.185 km/sec. The low-velocity (low energy) projectile extrudes and deforms the target and produces radial tears over a larger target area. During extrusion and deformation of a target, more projectile energy is dissipated than during target penetration by a higher velocity projectile. Figure 4 shows a target composed of 10 layers of spaced aluminum sheets. The target was impacted by a steel projectile with an impact velocity of 0.140 km/sec. Figure 4 clearly shows the variation of the perforation mechanism as the impact velocity of the projectile decreases. The perforations shown in figure 4 are caused primarily by shearing the small disks (or caps), which do not separate from the respective target sheets.

The results of high-energy and low-energy penetration of identical targets (as shown in figures 3 and 4), as well as the nonlinearity of the curves in figure 2, lead to the conclusion that the percent of projectile energy absorbed by the target during a single thin-sheet penetration decreases as the projectile velocity increases. A similar observation was made in tests conducted at the University of South Carolina (ref. 2).

The penetration of a 15-layer, loosely clamped laminate is shown in figure 5. The layers have been separated to show how the extrusion varies with each layer. The first layer shows very little deformation, because it was impacted by the projectile at a maximum velocity, and thus, the penetration of the first layer is similar to a single-sheet penetration. Layers 2 to 10 show more extrusion than is observed for a single-sheet penetration. This extrusion process is caused by the interaction among layers.

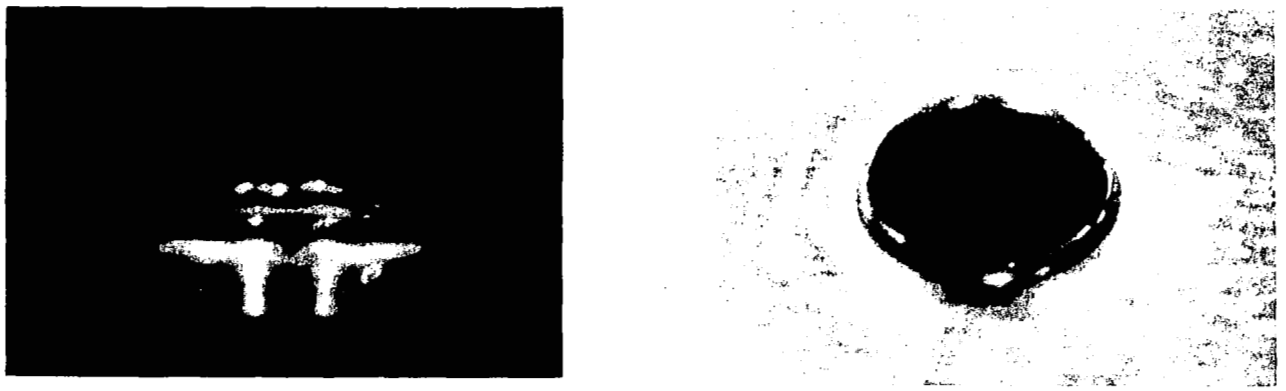

(a) Single layer perforated by a steel projectile with an impact velocity of 0.300 km/sec.

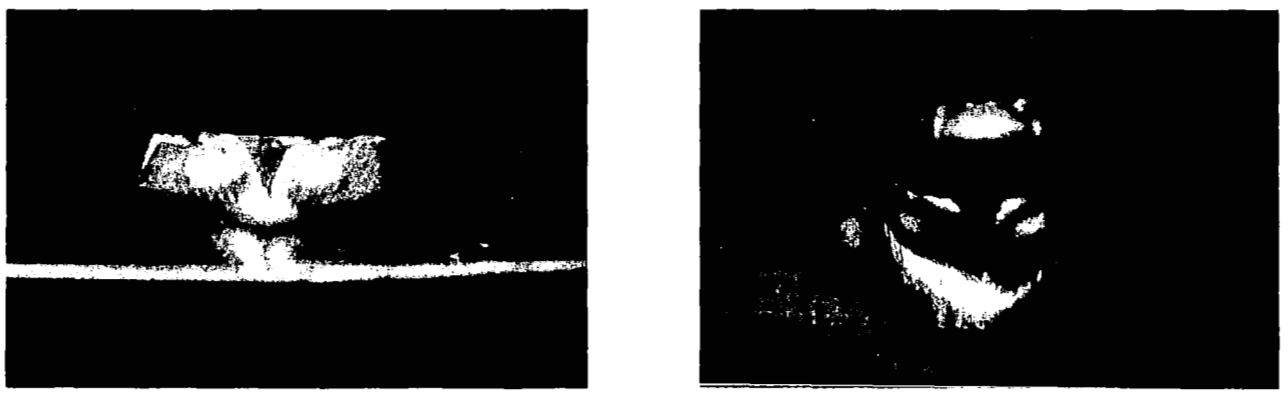

(b) Single layer perforated by a glass projectile with an impact velocity of 0.185 km/sec.

Figure 3.- Comparison of perforations of a single sheet of aluminum.

(a) Layer 1.

(b) Layer 2.

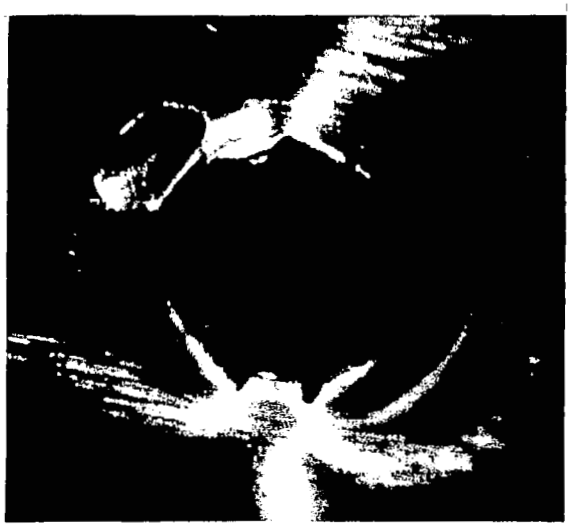

(c) Layer 3.

(d) Layer 4.

Figure 4. - Photomicrographs of the back surfaces of the layers of a target made up of 10 aluminum sheets. Layer 9 of the target was not completely penetrated by the projectile, but layer 9 was deformed more than the spacing between layers, which caused deformation of layer 10.

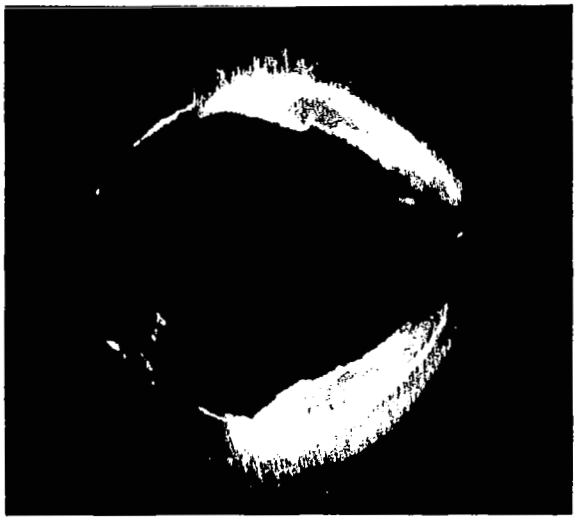

(e) Layer 5.

(f) Layer 6.

(g) Layer 7.

(h) Layer 8.

Figure 4. - Continued.

(i) Layer 9.

(j) Layer 10.

Figure 4. - Concluded.

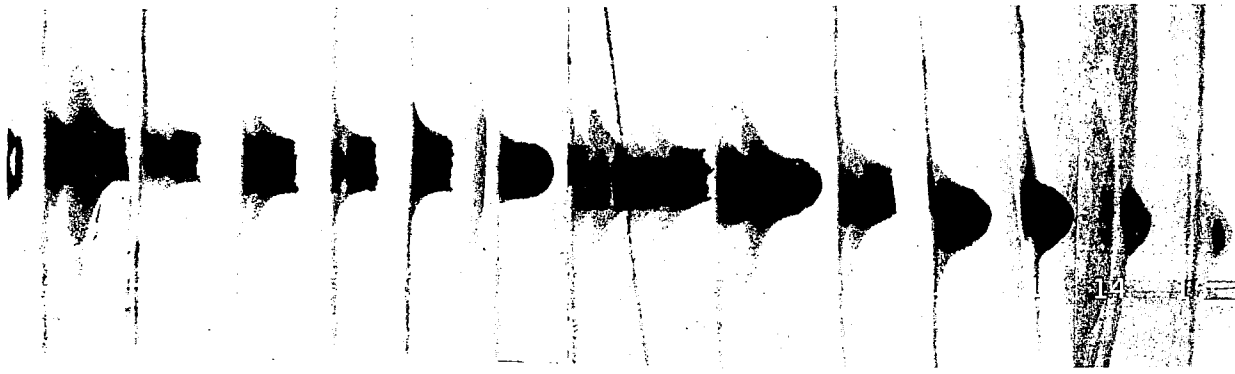

Figure 5. - Separated layers of a loosely clamped 15-layer target.

An explanation of the process is aided by the figure 6 sketches. Figures 6(a) to 6(c) represent an enlarged view of a projectile penetrating a loosely clamped multilayer target. As the projectile penetrates the first layers, the target interaction area is at a minimum, because projectile velocity is at its maximum. The inner layer progressively shows more deformation, because of the interactions with other layers and the buildup of small shear-caps on the projectile leading surface, as shown in figure 6(d). The size of a shear-cap is determined by the projectile velocity and the penetration process that occurs in that particular layer. As the projectile penetrates the inner layers of a target, the increasing resistance of multiple target layers squeezes the individual layers around the projectile. The target ductility also causes extrusion, and more of the adjacent target area reacts to the projectile than is normally expected for single-sheet penetration.

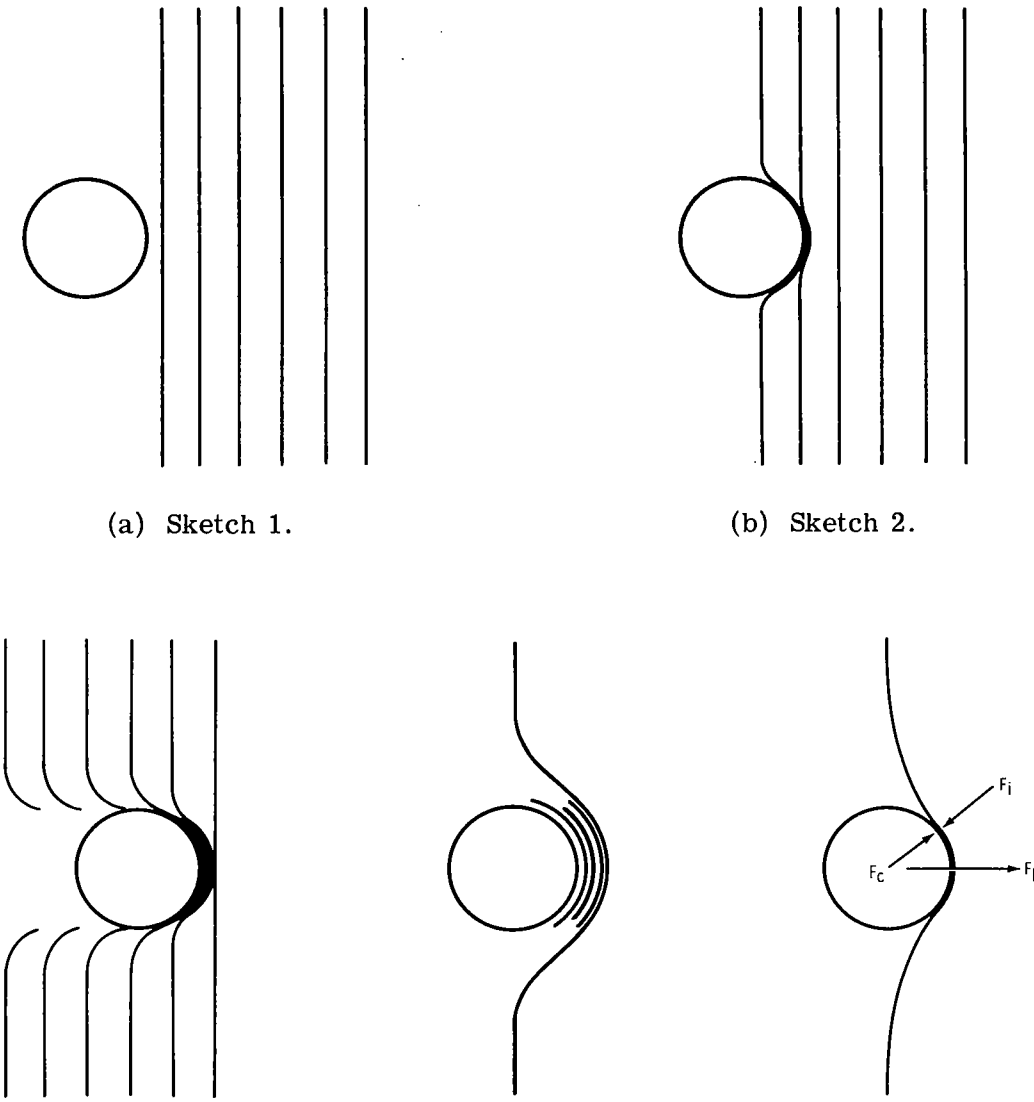

(a) Sketch 1. (b) Sketch 2.

(c) Sketch 3. (d) Sketch 4. (e) Sketch 5.

Figure 6. - The multilayer extrusion process.

The projectile penetration forces and the target resistance forces are shown in figure 6(e). The force F_i is the sum of the tension forces and the shear forces that resist projectile penetration; F_i may be time dependent. The force acting normal to the projectile-target interface is labeled F_c, which is a component of the total force F_p exerted by the forward motion of the projectile. The variation of these

forces from layer to layer causes the variation in the deformation of individual layers and the size variation of the plugs (or caps) sheared or extruded from the layers by the projectile.

An example of deformation for several layers is shown in figure 7. Several layers of the 15-layer target are shown magnified in figure 7(a). Caps that were removed from layer 10 when the target was separated are shown in figure 7(b). The caps are irregularly shaped, with the cap at the center of the photomicrograph still attached to the projectile. When the target layers were separated, the projectile was found wedged in layer 7. Caps were sheared from layers 1 to 11 and lodged in layers 10 and 12. Enlarged detail of the caps found in layer 10 is shown in figure 8. (Note the concentric circles, which are the peripheries of the caps.)

(a) Enlarged view of layers 7 to 11 of the 15-layer target.

(b) Caps removed from layer 10 of the 15-layer target.

Figure 7. - Enlarged view of layers 7 to 11 of the 15-layer target and the caps removed from layer 10.

(a) View of the downstream side of layer 10 with light coming from the upstream side.

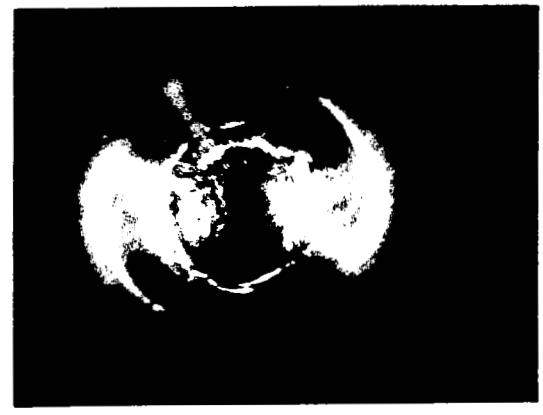

(b) View of the downstream side of layer 10 with light coming from the downstream side.

Figure 8. - Enlarged view of layer 10 of the 15-layer target.

(c) View of the upstream side of layer 10 with light coming from the upstream side.

Figure 8. - Concluded.

The target analysis is based on the ballistic limit. For thin-sheet aluminum, the ballistic limit is defined as the maximum impact velocity a projectile can have without producing fractures on the rear surface of the target. For spaced multisheet targets, such as the target shown in figure 4, the ballistic limit is readily determined, since all layers are completely penetrated, except for layer 10. This last sheet is damaged to various degrees, depending on the particular shot. If the ballistic limit for a single sheet is known, the ballistic limit for the entire target can be estimated. For the loosely clamped aluminum sheets, the velocity range was bracketed, because surface failure in the last sheet occurs over a wide velocity range.

The predictions of the low-velocity penetration equation developed by Bohn and Fuchs (ref. 3) for thick single-sheet targets and projectile velocities between 1 and 3 km/sec were compared with the experimental data. The equation is

$$\frac{t}{d_p} = \frac{2\rho_p}{\rho_t}\left[\ln(1 + A) - \frac{A}{1 + A}\right] \qquad (1)$$

where $A = 5.83V_p\sqrt{\rho_t/H}$

d_p = diameter of projectile, mm (in.)

H = Brinell hardness, kg/mm^2

t = target thickness, mm (in.)

V_p = projectile velocity, km/sec

ρ_p = projectile density, g/cm^3

ρ_t = target density, g/cm^3

The experimentally determined penetration depths are compared with the penetration depths predicted by the Bohn and Fuchs equation in figures 9 and 10. The theoretical depths are for single-sheet aluminum, and the wide divergence in slope indicates that the equation is not applicable to the target configurations used in these tests. The total penetrated thickness is determined by multiplying the ordinate of figures 9, 10, and 11 by 8.89×10^{-2} millimeters (3.5 mils) (the thickness of one aluminum sheet).

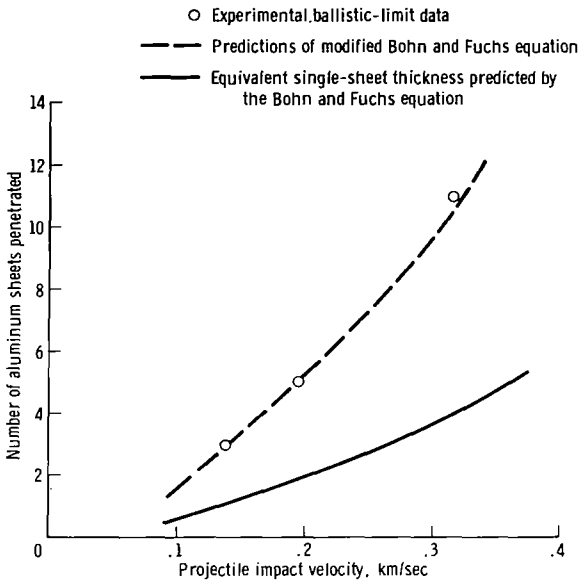

Figure 9. - Comparison of the predictions of the Bohn and Fuchs equation and the modified Bohn and Fuchs equation with experimental ballistic-limit data for glass projectiles impacting a layered target made up of aluminum sheets separated by 4.76 millimeters (three-sixteenths inch).

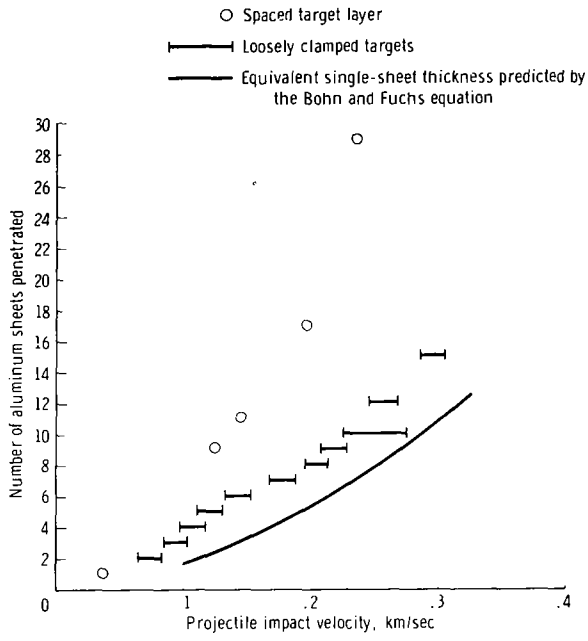

Figure 10. - Ballistic-limit data for a layered target made up of aluminum sheets. The target was impacted by steel projectiles.

The ratio k of the experimentally determined number of spaced layers penetrated by a glass projectile to the number of layers required for an equivalent single-sheet thickness to be penetrated as predicted by Bohn and Fuchs equation has an average value of 2.72. The number of layers penetrated as a function of the projectile impact velocity, as predicted by the Bohn and Fuchs equation, is shown by the solid line in figure 9. If this theoretical curve is multiplied by 2.72, the dashed line in figure 9 results. The dashed line in figure 9 is in good agreement with experimental data. The form of the Bohn and Fuchs equation (eq. (1)) represented by the solid line in figure 9 is

$$N = 58.2\left[\ln (1 + A) - \frac{A}{1 + A}\right] \tag{2}$$

where $N = t(mm)/8.89 \times 10^{-2}$ mm or $t(in.)/3.5 \times 10^{-3}$ in., and the values to obtain equation (2) are $\rho_p = 2.2$ g/cm^3, $\rho_t = 2.7$ g/cm^3, $H = 40$ kg/mm^2, and $d_p = 3.175$ mm (0.125 in.). The equation for the dashed line in figure 9 is

$$N = 158.3\left[\ln (1 + A) - \frac{A}{1 + A}\right] \tag{3}$$

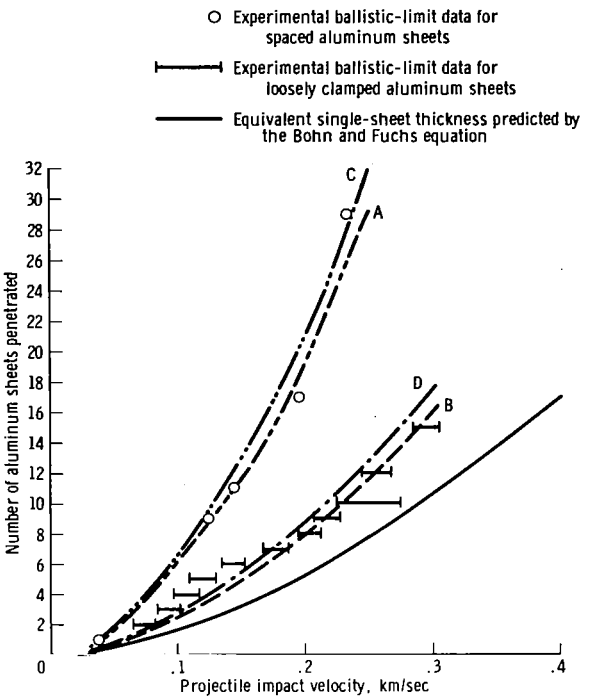

Figure 11. - Comparison of the Bohn and Fuchs equation with the experimental ballistic-limit data for a layered target made up of aluminum sheets. The target was impacted by steel projectiles.

Modifying the original Bohn and Fuchs equation gives

$$t = 0.554\left[\ln(1 + A) - \frac{A}{1 + A}\right] \qquad (4)$$

The number of spaced layers penetrated by a steel projectile, as predicted by the Bohn and Fuchs equation, is shown by the solid line in figure 10. Curves A and B of figure 11 are the theoretical curve multiplied by the k-values of 3.66 and 1.5, respectively, which are the constants determined for steel-projectile impacts into spaced and loosely clamped targets, respectively. These constants change the original Bohn and Fuchs equation to

$$t = 2.6\left[\ln(1 + A) - \frac{A}{1 + A}\right] \quad \text{(for spaced layers)} \qquad (5)$$

and

$$t = 1.07\left[\ln(1 + A) - \frac{A}{1 + A}\right] \quad \text{(for loosely clamped layers)} \qquad (6)$$

where $\rho_p = 7.7\ \text{g/cm}^3$

$\rho_t = 2.7\ \text{g/cm}^3$

$H = 40\ \text{kg/mm}^2$

Curves C and D show slightly larger constants, 4.0 and 1.65, respectively. Attempts to relate these constants to a fractional exponent of ρ_p have been unsuccessful. More data are needed for varying target densities and projectile diameters for the general case to be determined.

TEXTILE MATERIALS

Cloth materials have also been impacted with low-velocity projectiles in order to determine their resistance to penetration and, thus, usefulness as space-suit materials. For textile materials, the ballistic limit is defined as the maximum velocity with which a given projectile can impact a target without perforating the target. The ballistic limit is also bracketed for nylon cloth, because the velocity data vary as a function of projectile impact position relative to the weave. Table II is a comparison of the experimentally determined ballistic limits of woven nylon of various area densities. Unfortunately, the area-density variation is accomplished by changing the thread size, thread compactness (threads/inch), and type of weave. The ballistic limits of these materials are functions of material density, elasticity and yield strength of individual threads, and position of impact on the weave; therefore, the correlation among data points is very limited. Of the entire group tested, the 0.1791-kg/m^2 (6.04 oz/yd^2) nylon has the highest ballistic limit and, therefore, is the most efficient low-velocity-projectile energy-absorber material tested.

TABLE II. - BALLISTIC LIMIT FOR LAYERED NYLON OF VARYING AREA DENSITY

Area density of material		Layers of material tested	Ballistic limit, km/sec
kg/m^2	oz/yd^2		
0.082	2.78	1	0.10 to 0.11
		2	.14 to 0.185
		3	.177 to 0.185
.154	5.21	1	.15 to 0.162
.1791	6.04	1	.195 to 0.215
		2	.322 to 0.337
		3	>0.38
.246	8.3	1	.172 to 0.185
		2	.22 to 0.28
.415	14	1	.18 to 0.195
		2	.22 to 0.23

The photographs in figures 12 and 13 show the relative size of the projectile to the thread diameter and weave, as the area density of the cloth varies. (All the samples are made from type HT-1 nylon (Nomex).) Of the nylon samples tested, the most effective barrier is the weave and thread size that presents the most dense homogeneous surface to the impacting projectile.

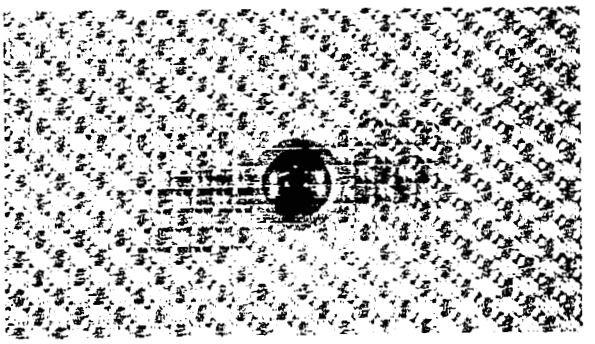

(a) Area density, 0.246 kg/m^2 (8.3 oz/yd^2).

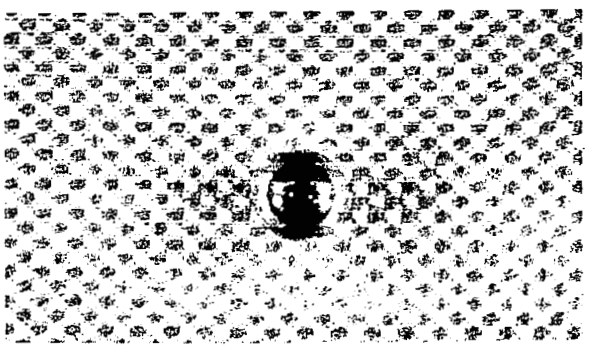

(b) Area density, 0.154 kg/m^2 (5.21 oz/yd^2).

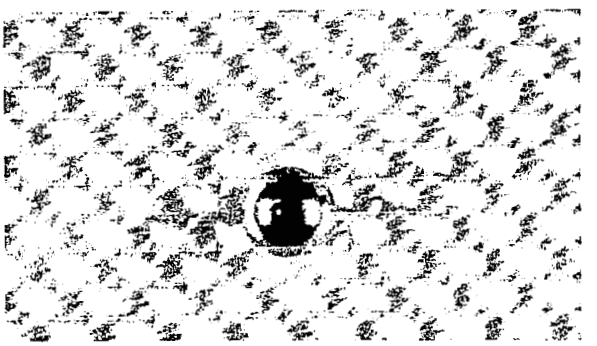

(c) Area density, 0.415 kg/m^2 (14 oz/yd^2).

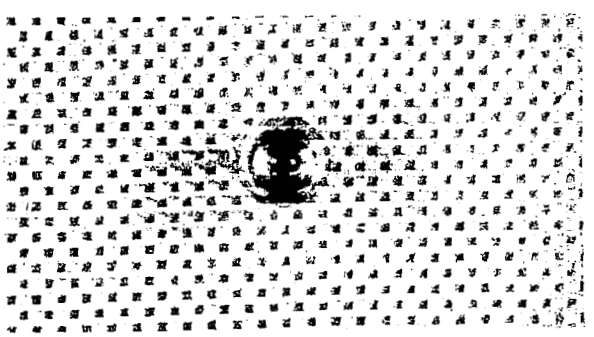

(d) Area density, 0.1791 kg/m^2 (6.04 oz/yd^2).

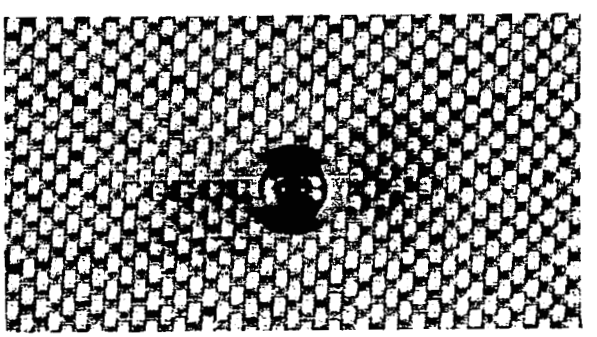

(e) Area density, 0.082 kg/m^2 (2.78 oz/yd^2).

Figure 12. - Comparison of nylon weave, thread size, and thread density with the steel projectile.

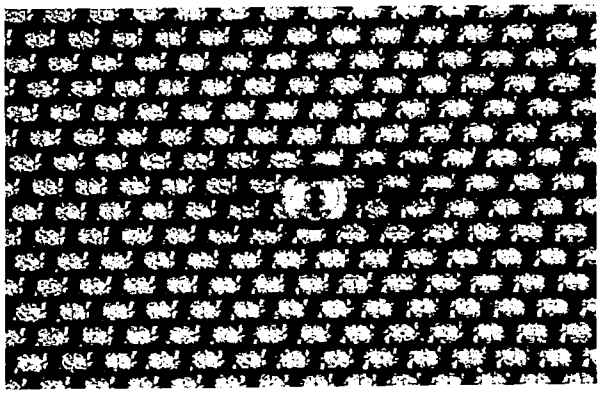

(a) Area density, 0.4152 kg/m^2 (14 oz/yd^2); silicone treated.

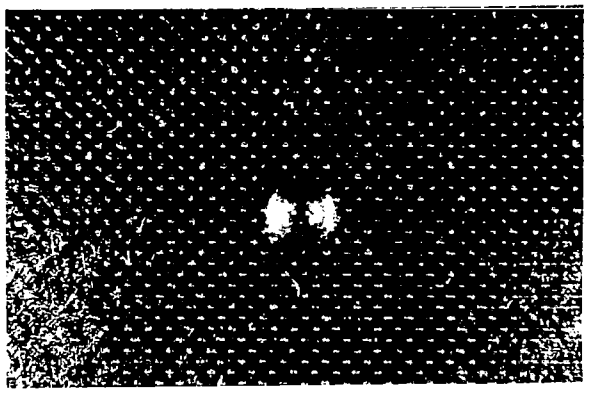

(b) Area density, 0.1426 kg/m^2 (4.82 oz/yd^2); aluminized.

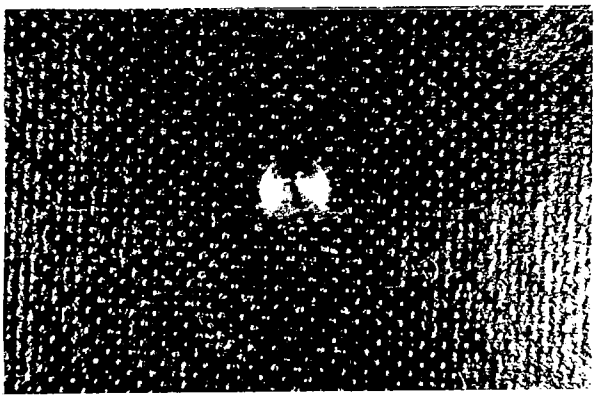

(c) Area density, 0.1794 kg/m^2 (6.05 oz/yd^2); aluminized.

Figure 13. - Comparison of treated nylon weave, thread size, and thread density with the steel projectile.

The effect of chemical treatment, or surface coating, on the penetration resistance of nylon cloth was also tested with low-velocity projectiles. The results indicate that any treatment or coating that tends to bond the threads together and force a larger sample area to react to an impact will increase the penetration resistance. However, the bonding must be accomplished without interfering with the elasticity and strength of the nylon, because the projectile energy is absorbed as the nylon is stretched and deformed. The results of the impact tests of treated nylon cloth are shown in table III.

It should be noted that aluminized woven nylon materials have decreased resistance to low-velocity penetration. For the single-layer samples tested, the ballistic limit was reduced by approximately 25 percent; and for two-layer samples, the ballistic limit was reduced by approximately 50 percent. These values were obtained for the 0.1794-kg/m^2 (6.05 oz/yd^2) aluminized nylon and the 0.1791-kg/m^2 (6.04 oz/yd^2) untreated nylon. The substantial decrease in penetration resistance is attributed to the effect of the aluminum on the strength and ductility of the individual strands in the material.

TABLE III. - BALLISTIC LIMIT OF VARIOUS WOVEN SAMPLES

AND SAMPLE CONFIGURATIONS

Area density of material		Description of material	Layers of material tested	Ballistic limit, km/sec
kg/m^2	oz/yd^2			
0.142	4.8	Aluminized nylon	1	0.125 to 0.140
			2	.177 to 0.20
.1794	6.05	Aluminized nylon	1	.14 to 0.16
			2	.18 to 0.19
.415	14	Ballistic nylon, waterproofed with silicone	1	.172 to 0.185
			2	.29 to 0.30
.163	5.5	Nylon and Mylar laminate	[a]2	.12 to 0.132
			[b]2	.14 to 0.15
.082	2.78	Nylon and nylon laminate	[c]2	.18 to 0.195
.1791	6.04		[d]2	.2 to 0.21

[a]The projectile impacted on the Mylar side of the laminate.

[b]The projectile impacted on the nylon side of the laminate.

[c]The projectile impacted on the 0.082-kg/m^2 (2.78 oz/yd^2) nylon side of the target.

[d]The projectile impacted on the 0.1791-kg/m^2 (6.04 oz/yd^2) nylon side of the target.

Multilayers of waterproofed silicone-treated nylon have more resistance to low-velocity penetration than untreated multilayers of nylon. This resistance is attributed to the silicone binding of the nylon threads, which gives the cloth material a larger interaction area during the impact deformation. For the untreated nylon with similar weave and identical density of 0.415 kg/m^2 (14 oz/yd^2), the projectile interaction area is small. In effect, the projectile squeezes through the weave without breaking any

threads. This resistance to penetration does not happen as readily with the silicone-treated nylon. A 0.163-kg/m^2 (5.5 oz/yd^2) nylon and Mylar laminate was tested with projectile impacts on both sides. It was found that the sample had more resistance to penetration when the woven nylon surfaces were impacted first, with the Mylar on the downstream side. This result is attributed to the Mylar forcing more material to react to the impact. The Mylar bonds the threads together, but still permits them to stretch.

The nylon-cloth samples were retested in multilayer combinations of various area densities to determine the minimum density combination that would stop a steel projectile with an impact velocity of 0.200 km/sec. The most efficient of the samples is the combination of 0.082-kg/m^2 (2.78 oz/yd^2) and 0.1791-kg/m^2 (6.04 oz/yd^2) nylon, when the lower density material is impacted first. Figures 14 and 15 are photographs of the damage to this combination when it is impacted from either side. In figure 15, the large interaction area on the 0.082-kg/m^2 (2.78 oz/yd^2) material should be noted.

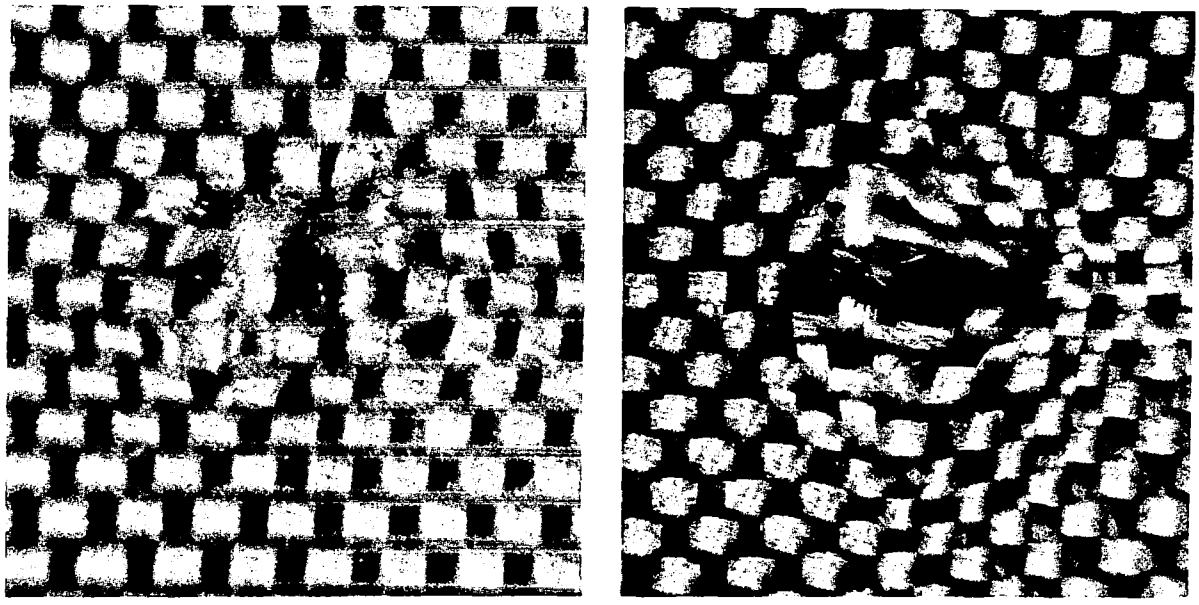

(a) First layer impacted; area density, 0.1791 kg/m^2 (6.04 oz/yd^2).

(b) Second layer impacted; area density, 0.082 kg/m^2 (2.78 oz/yd^2).

Figure 14. - Damage to a double-layer nylon target impacted (material with higher area density impacted first) by a steel projectile with an impact velocity of 0.200 km/sec.

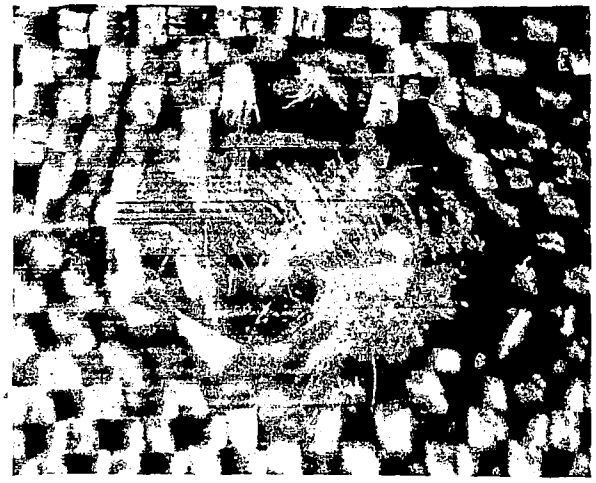

(a) First layer impacted; area density, 0.082 kg/m^2 (2.78 oz/yd^2).

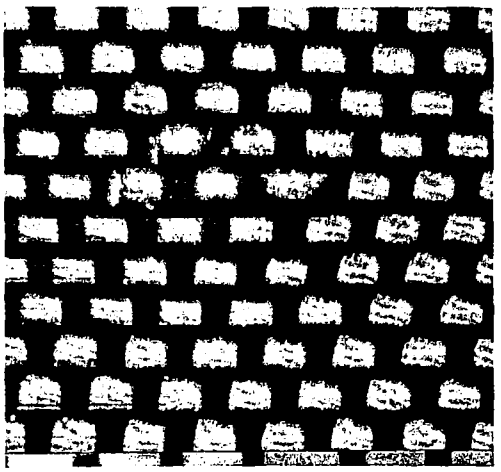

(b) Second layer impacted; area density, 0.1791 kg/m^2 (6.04 oz/yd^2).

Figure 15. - Damage to a double-layer nylon target impacted (material with lower area density impacted first) by a steel projectile with an impact velocity of 0.200 km/sec.

CONCLUSIONS

The results of the study described in this report indicate that steps can be taken to substantially reduce the hazard from secondary-meteoroid impact, which might occur on or near the lunar surface. In the design of spacecraft, space suits, and structures for the lunar and near-lunar environment, a selection of materials and material configurations can be made that will decrease the low-velocity-particle penetration hazard, without increasing the weight or volume of the structure.

The impact tests described in this report indicate the following.

1. Loosely clamped thin aluminum sheets form a more efficient low-velocity-particle absorber than spaced sheets do.

2. The percent of total particle energy absorbed by a given thin sheet decreases as the incident velocity increases, because the projectile-target interaction occurs over a smaller area of the target when the impact velocity is large.

3. The Bohn and Fuchs penetration equation is adequate for predicting the penetration of small, low-velocity projectiles in thin multilayer aluminum targets if the appropriate ratio of the number of spaced layers penetrated to the number of layers required for an equivalent single-sheet thickness to be penetrated is determined.

4. Preliminary investigation indicates that a ratio of the number of spaced layers penetrated to the number of layers required for an equivalent single-sheet thickness to be penetrated can be determined for woven nylon fabrics of varying area density. A tight compact weave is the most efficient energy absorber.

5. The multilayer silicone-treated ballistic nylon is a more efficient energy absorber than untreated multilayers of nylon.

6. Layered targets composed of variable-density materials can be made more efficient energy absorbers if the layers are arranged with the higher density materials on the downstream side of the target.

Manned Spacecraft Center
National Aeronautics and Space Administration
Houston, Texas, February 10, 1971
914-50-18-22-72

REFERENCES

1. Cour-Palais, B. G.; et al.: Meteoroid Environment Model - 1969 [Near Earth to Lunar Surface]. NASA SP-8013, Mar. 1969.

2. French, A. P.: Dissipation of Projectile Energy on Impact, Final Report. Note 11-57-P1, University of South Carolina, Department of Physics, 1957.

3. Bohn, J. Lloyd; and Fuchs, Otto P.: High Velocity Impact Studies Directed Towards the Determination of the Spatial Density, Mass and Velocity of Micrometeorites at High Altitudes. Scientific Report No. 1, Temple University, Philadelphia, Contract AF 19(604)-1894, Jan. 31, 1958.

NASA-Langley, 1971 — 17 S-238